Chemical Engineering Science 113 (2014) 35–44

Contents lists available at ScienceDirect

Chemical Engineering Science

journal homepage: www.elsevier.com/locate/ces

Effect of ultrasound on mass transfer during electrodeposition for electrodes separated by a narrow gap

S. Coleman *, S. Roy

School of Chemical Engineering and Advanced Materials, Newcastle University, Merz Court, Newcastle upon Tyne, England NE1 7RU, UK

HIGHLIGHTS

- Mass transfer during electrodeposition using side-on ultrasonic agitation is studied.
- Narrow electrode gaps and limitations of the limiting current technique are examined.
- Mass transfer correlation is developed for the side-on system for a narrow gap.
- Developed and fully turbulent flows were found for narrow and large gaps respectively.
- Distortions in polarization data is caused by close placement of ultrasonic probe.

ARTICLE INFO

Article history:
Received 3 December 2013
Received in revised form
26 March 2014
Accepted 27 March 2014
Available online 4 April 2014

Keywords:
Electrodeposition
Ultrasonic agitation
Enface Technique
Mass transfer correlation
Limiting current

ABSTRACT

This work reports an investigation on mass transfer by ultrasound agitation during electrodeposition on electrodes separated by a narrow inter-electrode gap. Polarisation experiments were performed to identify the mass transfer limiting current. The limiting current density was used to calculate mass transfer boundary layer thicknesses which were used to develop mass transfer correlations. Experiments were carried out using a cell with parallel copper discs which were positioned at gaps of 1, 0.5 and 0.15 cm. The distance between the ultrasonic probe and electrodes was varied between 3 and 1.5 cm. The polarisation data showed clear limiting current plateaux when the distance between the electrodes was larger, however significant distortions were observed when the gap was 0.15 cm. It was found that lower ultrasound powers of 9–18 W/cm^2 provided more effective agitation at narrower electrode gaps than powers exceeding 18 W/cm^2. Sherwood correlations showed that in this system, developing turbulence occurs for larger inter-electrode spacing, whereas for narrow electrode gaps fully turbulent correlations were obtained. A 2-D current distribution model showed that potential distortions that were observed in the polarisation data were caused by the close placement of the metallic US probe to the two parallel electrodes.

1. Introduction

Microfabrication has a variety of applications, including fabrication of MEMS, microfluidics and micro-optic systems (Franssila, 2010; Madou, 2012). The widespread use of these products has led to the search for new microfabrication processes (Doraiswamy et al., 2009; Samarasinghe et al., 2006; Whitaker et al., 2005; Yu et al., 2006). One such method is an electrochemical process, called EnFace (Roy, 2007). The process can selectively etch or plate metal at the microscale, using a patterned tool placed in close proximity to the substrate surface, when a voltage or current is passed between them. Experimentally, it was shown that copper patterns ranging between 5 and 100 μm can be successfully etched (Schonenberger and Roy, 2005) or deposited (Wu et al., 2011) using a vertical flow-by system.

Since the technique required inter-electrode gaps of less than 500 μm, forced convection flow was needed to assist with species transport to and from the electrode surface. Furthermore, modelling studies showed that both forced convection flow within the inter-electrode gap was a crucial parameter in controlling the ability of pattern transfer (Nouraei and Roy, 2008; Wu et al., 2011). Due to the issues associated with scaling up such a cell, the ability to etch or plate at the microscale was also investigated using a conventional beaker-type geometry. However, implementing Enface in a non-agitated beaker system restricted the mass transfer of ionic species within the inter-electrode gap (Widayatno and Roy,

* Corresponding author.
E-mail address: simon.coleman@ncl.ac.uk (S. Coleman).

http://dx.doi.org/10.1016/j.ces.2014.03.026

2011). This investigation established that a method which directs agitation towards the narrow gap was required.

It is well known that a diffusion layer forms at an electrode surface; if the reaction is carried out for short periods of time when diffusion is the dominant transport mechanism, then classical equations developed by Cottrell (1903) and Sand (1901) may be used. If the reaction results in a movement of ions in the bulk leading to natural convection flow formation, then laminar or turbulent correlations for free convection, such as Eq. (1-a) (Wagner, 1949) and (1-b) (Fouad and Ibl, 1960) respectively, may be used.

$$Sh = 0.67(Gr\,Sc)^{1/4} \quad (1-\mathrm{a})$$

$$Sh = 0.31(Gr\,Sc)^{0.28} \quad (1-\mathrm{b})$$

Alternatively, agitation can be provided via forced convection flow and corresponding Sherwood number correlations, such as Eq. (2) can be used (Tobias and Hickman, 1965).

$$Sh = 0.85\left(Re\,Sc\,\frac{d_e}{L}\right)^{1/3} \quad (2)$$

For the case of turbulent flow between two parallel plates the general Sherwood number correlation is

$$Sh = a\left(Re\,Sc\,\frac{d_e}{L}\right)^{b} \quad (3)$$

$0.7 < b < 0.8$ for developing turbulent flow
$b > 0.8$ for fully developed turbulent flow

While these equations have been used extensively (Wragg, 1971; Wragg and Ross, 1967), they are valid only when the two electrodes are sufficiently far from each other, and no interaction of boundary-layer takes place.

In fact, few mass transfer correlations exist for forced convection between parallel electrodes are separated by a narrow gap. Although several studies on electrochemical growth (Kuhn and Argoul, 1995), surface adsorption (Texier et al., 1998) and analysis (Compton et al., 1996b; Tolmachev et al., 1996) have been carried out using a horizontal channel cell with a thin gap, this system has never been used for practical electrodeposition purposes. Where steady state electrochemical deposition has been performed, it has been shown that electrochemical reactions within narrow gaps can lead to instabilities in material transport (Rosso et al., 2002; Zelinsky and Pirogov, 2009). For example, silver deposition onto silver electrodes separated by a narrow gap of 1 mm in 0.01 M $AgClO_4$ electrolyte showed oscillations in the transfer of ions due to the constriction of boundary layers near the electrode surface (Zelinsky and Pirogov, 2009). Copper electrodeposition from 0.1 M $CuSO_4$ at parallel plates with an inter-electrode distance of 8 mm also exhibited concentration instabilities as the mass transport limit was approached (Rosso et al., 2002). Both these studies confirmed that such thin gap cells are unsuitable for electrodeposition due to mass transfer limitations.

Ultrasonics (US) is a forceful form of agitation which can improve stirring in electrochemical systems (Compton et al., 1996a; Walton et al., 1995). An ultrasonic transducer is a vibrating solid that can induce ultrasound waves through a solution which can result in cavitation. It is suggested that cavitation phenomena contributes to the enhancement of stirring (Compton et al., 1996a; Maisonhaute et al., 2001; Mason and Lorimer, 2002; Ohsaka et al., 2010; Ramachandran and Saraswathi, 2009; Richardson et al., 1997; Walton et al., 1995; Yeager and Hovorka, 1953). Much of the research work has established the improvement of mass transfer in electrodes which are far away from each other (Compton et al., 1996a; Lorimer et al., 1996; Marken et al., 1996; Ramachandran and Saraswathi, 2009), but no information is available for cases where there is a narrow gap between parallel plates.

The effect of US agitation has been most extensively studied by probes orientated face-on to the working electrode surface (Compton et al., 1996a; Marken et al., 1996; Ramachandran and Saraswathi, 2009), illustrated in Fig. 1(a). A study using this orientation, with a reduction of $Ru(NH_3)_6^{3+}$ at the working electrode for example, demonstrated the importance of the distance from the probe tip to the centre of the electrode surface (d_p), showing that the limiting current (i_{Lim}) is approximately $i_{Lim} \propto 1/{d_p}^{1/3}$ (Marken et al., 1996). This was attributed to the narrower jet of flow close to the probe tip compared to distances further away (Marken et al., 1996), thereby increasing the intensity of the mixing at the electrode surface as the tip is brought closer to it. The effect of the US power intensity on mass transfer has also been investigated (Compton et al., 1996a; Lorimer et al., 1996; Ramachandran and Saraswathi, 2009). For instance, with a study of a $K_4Fe(CN)_4$ redox reaction at a glassy carbon electrode, varying the power intensity (p) showed that the diffusion layer thickness (δ) is approximately $\delta \propto 1/p^{1/3}$ (Compton et al., 1996a). These investigations illustrated the importance of choosing appropriate US parameters to influence mass transfer in electrochemical systems.

To these authors' knowledge only one investigation has been carried out on the effect of ultrasound variables in the side-on geometry (Eklund et al., 1996), displayed in Fig. 1(b). This investigation studied the effect of the 'side-on' probe on the mass transfer during the oxidation of ferrocene at a platinum plate electrode. The researchers developed a theoretical analysis based on earlier forced convection systems where the fluid flowed past the electrodes (Levich, 1962). They established that agitation conditions could be analysed using such a model, and that the diffusion layer across the surface of the electrode was non-uniform and had thicknesses of 10–12 μm at the downstream edge of the electrode (Eklund et al., 1996).

At this point the effectiveness of US agitation to enable mass transport within two parallel plates, as illustrated in Fig. 1(c), has remained unexplored. In this work, we have attempted to quantitatively assess the effect of US agitation on mass transfer during electrochemical metal deposition in a system with a combined geometry of a 'side-on' probe and narrow inter-electrode gap. A well-established limiting current technique, widely used for determining material transport, is employed to determine the thickness of mass transfer boundary layers. The electrochemical system is copper deposition from acidified 0.1 M $CuSO_4$ solutions, where flow instabilities have been encountered (Rosso et al., 2002). We have measured the limiting current for copper deposition with and without US agitation. Limiting currents have been used to calculate the mass transfer boundary layer thickness, and Sherwood number correlations have been developed. Experiments have been carried out using a small cell where parallel electrodes at gaps of 1, 0.5 and 0.15 cm have been placed. The gap between the US probe and electrodes has been varied between 3 and 1.5 cm. The usefulness of utilizing the limiting current method, which is often carried out to determine mass transfer boundary layer thickness during electroplating, has been critically examined, particularly for the case of narrow electrode geometries.

2. Theory

It is suggested that the flow regime from an ultrasound probe tip is similar to a turbulent jet of flow from a pipe of the same diameter (Marken et al., 1996). Furthermore, Eklund et al. (1996) proposed that the flow of ultrasound waves over an electrode surface from a 'side-on' probe is analogous to flow over a plate.

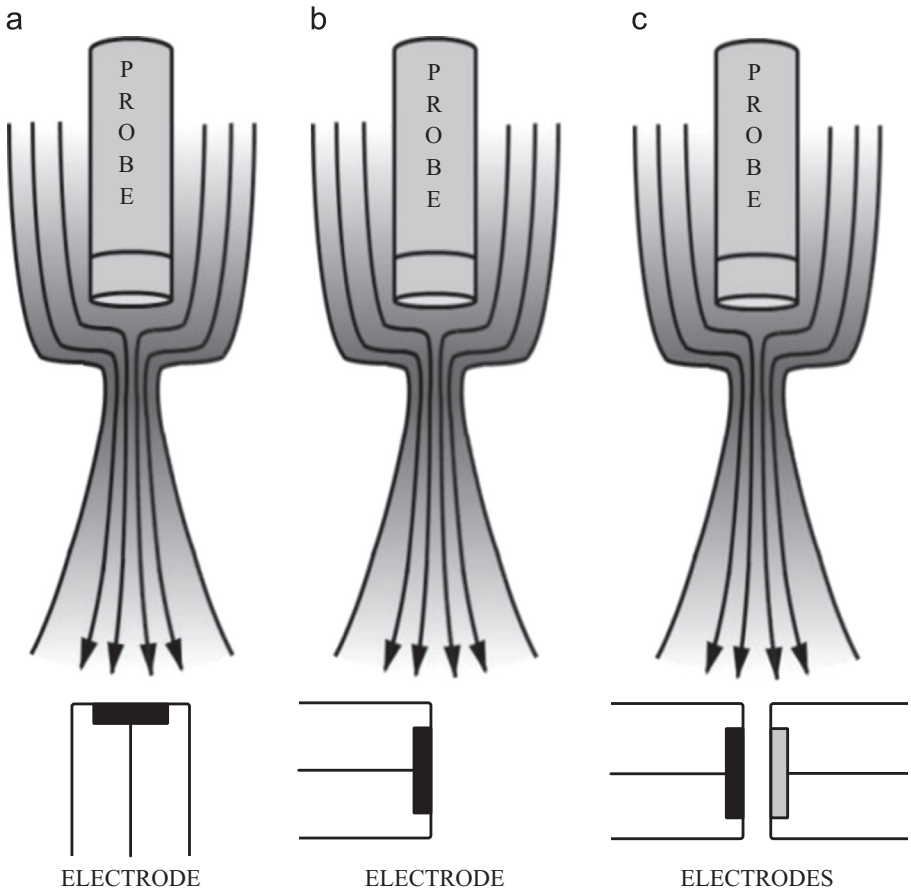

Fig. 1. US probe orientations relative to an electrode. (a) face-on; (b) side-on; and (c) side-on with narrow electrode gap. Adapted from Marken et al. (1996).

Based on this assumption, these researchers used an analysis proposed by Levich (1962) for forced convection. They derived Eq. (4) to describe the limiting current at an electrode when such a forced US agitation takes place for a side-on arrangement (Eklund et al., 1996).

$$I_{sono} = \frac{0.34FD^{2/3}U^{1/2}wc_b}{\nu^{1/6}} \times \int_{h_0}^{h_0+2r} \frac{1}{x^{1/2}[1-(h_0/x)^{1/3}]^{1/3}}\,dx \qquad (4)$$

In Eq. (4), F, D, c_b and ν are the Faraday constant, diffusion coefficient, bulk concentration of reacting species and the kinematic viscosity respectively. The parameter w is the width of the electrode, and the parameter x is the distance along the length of the electrode from the edge closest to the probe. In Eq. (4) h_0 is the distance between the leading edge of the momentum and the concentration boundary layers. The limits of the integral are set at h_0 and h_0+2r since the deposition reaction occurs at the metal surface (c.f. Fig. 3c).

The only unknown parameter in the equation is U, the velocity of the flow far away from the electrode surface. For US agitation, U is related to the ultrasound power and is the limiting solution velocity at a large distance from the plate. The effect of bringing the probe tip closer is governed by changing the parameter 'd_p', which is defined as the distance between the centre of the electrode to the US probe tip. It has been shown in earlier experiments that a distance between the probe and electrode of >3 cm is sufficiently far from the electrode surface for Eq. (4) to hold (Compton et al., 1996a; Eklund et al., 1996).

Eklund et al. (1996) carried out experiments using a 20 kHz probe placed side-on and 34 mm away from a platinum plate electrode where ferrocene was oxidised electrochemically. Experimentally measured limiting currents were used to calculate values of U using Eq. (4) at various ultrasound intensities. This analysis showed that U was linearly proportional to US power, which is displayed in Fig. 2. This proved that 'flow over a plate' was a reasonable model for this side-on probe system.

3. Methodology

Experiments were carried out in a 500 ml cylindrical PVC cell with two polished copper discs 1 cm in diameter acting as a cathode and anode, and faced each other separated by an electrode gap (Fig. 3). The distance between the electrodes was altered from 0.15 cm to 1 cm with the use of screw gauges on each electrode holder. The reference electrode was a copper wire wrapped in PTFE tape with only the tip exposed, placed approximately 0.5 cm from the cathode surface, above and to the side of the electrode gap. Copper is a stable reference electrode in acidified $CuSO_4$ electrolytes, and has been used previously for the measurement of polarisation data (Meuleman and Roy, 2003; Roy et al., 2001). The electrolyte solution used was an acidic electrolyte of 0.1 M $CuSO_4$+0.1 M H_2SO_4.

An *Eco Chemie Autolab Potentiostat (PGSTAT30)* was used to apply linear cathodic potential scans and *NOVA 1.7* software was used to input scan settings and record the response data. The ultrasonic

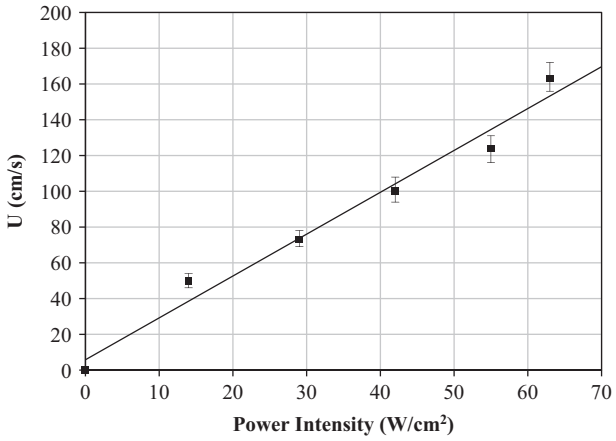

Fig. 2. A graph of U (best-fit value) obtained from the data (black square) published by Eklund et al. (1996). The distance between the probe and the centre of the electrode was 34 mm.

equipment used was a *SONICS Vibra-Cell VC505 Processor* connected to a 20 kHz ultrasound probe with a 1.3 cm diameter titanium alloy tip and was operated within a power range of 9–29 W/cm^2. The probe was placed above the gap in a side-on orientation (Fig. 3), with $d_p = 1.5$–3 cm. The probe tip was submerged into the solution by 0.4 cm for every probe–electrode distance.

The limiting current technique is based on the identification of limiting current plateaux from standard electrode polarisation data. For any electrochemical reduction reaction, current changes with potential, until it reaches the region where the reaction is mass transfer controlled. In this region the current becomes independent of the applied electrode potential, and a current plateau is observed in the polarisation data. This value of current, termed as the mass transfer limiting current, is related to the diffusion layer thickness. The limiting current density can be used to calculate the diffusion layer thickness from Eq. (5).

$$i_{Lim} = \frac{zFD(c_b)}{\delta} \tag{5}$$

In Eq. (5), z is the charge on the reacting species, D is the diffusivity of the reacting species and δ is the diffusion layer thickness. The value of δ was calculated using the Cu^{2+} ion concentration stated in the experimental section and a diffusion coefficient of 7.07×10^{-6} cm^2/s calculated using equations from Fenech and Tobias (1960).

The values of δ values calculated from the limiting current experiments were used to develop Sherwood number correlations. Sh numbers were calculated by the equation $Sh = L/\delta$ where L is the characteristic length, in this case $2r = 1$ cm, where r is the radius of the electrode (c.f. Fig. 8). The Sc number was calculated by $Sc = \nu/D$ where a kinematic viscosity (ν) of 1.004×10^{-2} cm^2/s was used and the diffusivity (D) was the same as was used in the limiting current calculations. The value of Re was based on the hydraulic diameter (d_H), which was used to calculate the equivalent diameter (d_e). The exact procedure is stated in the Appendix.

4. Results

Fig. 4a–c show the linear polarization scans for copper deposition at the cathode substrate using US agitation. Limiting current plateaux are observed as expected during copper deposition, although the data for lower probe–electrode distances and narrow electrode gaps exhibit smaller plateaux regions, resulting in a difficulty in measurement of the limiting current density (i_{Lim}). This measurement was also made more difficult due to noisy current fluctuations caused by cavitation bubble oscillations and micro-jetting resulting in sudden current peaks, which have been previously observed in side-on (Eklund et al., 1996) as well as face-on (Compton et al., 1996a; Marken et al., 1996) and probe arrangements. Figs. 4b and c, where probe–electrode distance or inter-electrode gap are small, show that hydrogen discharge potentials apparently occur at lower potentials, which makes detection of limiting current difficult.

The values of i_{Lim} for an inter-electrode gap of 1 cm (Fig. 4a) are in the range -57 to -130 mA/cm^2. This value is significantly greater than the i_{Lim} value measured separately under silent conditions, which was recorded at -10.5 mA/cm^2 respectively. This shows that agitation provided by ultrasound significantly increases the rate of mass transfer of Cu^{2+} ions towards the substrate. This enhancement in limiting current density with increasing US intensity has been previously reported in sonoelectrochemical investigations in the side-on (Eklund et al., 1996) and face-on geometry (Compton et al., 1996a; Ramachandran and Saraswathi, 2009).

Fig. 4b displays linear potential scans under ultrasound conditions for a narrower inter-electrode gap and varying probe–electrode distances. The value of i_{Lim} at an inter-electrode gap of 0.5 cm is approximately 90, 122 and 140 mA/cm^2 for the probe–electrode distances of 3, 2 and 1.5 cm respectively illustrating the increase in mass transfer as the probe is brought closer towards the electrode, evident in previous ultrasound investigations where the probe–electrode distance is varied (Compton et al., 1996a; Marken et al., 1996; Ramachandran and Saraswathi, 2009). It is suggested that this is due to the presence of a higher flow velocity at shorter distances from the probe tip (Marken et al., 1996).

Fig. 4c displays linear potential scans under ultrasound conditions for an even narrower inter-electrode gap and varying probe–electrode distances. The value of i_{Lim} remains virtually unchanged when the electrode spacing is decreased from 0.5 to 0.15 cm, demonstrating that ultrasound is an effective form of agitation even for narrow electrode gaps. However, the polarisation data are significantly different when using the narrower gap, i.e. 0.15 cm, being distorted, with a very small plateaux region.

The i_{Lim} values from polarization data were used with Eq. (4) to calculate the average thickness of the diffusion layer (δ) at the cathode at varying US powers and inter-electrode distances of 1 cm (large) and 0.15 cm (small), displayed in Fig. 5. These values of diffusion layer thickness are calculated for a probe–electrode distance of 3 cm, which can be deemed to be sufficiently far from the electrode surface.

As expected, the boundary layer is larger at lower US intensities compared to higher intensities for the case for the constant electrode separation of 1 cm. Narrowing the inter-electrode gap from 1 cm to 0.15 cm increases the δ due to constriction of convection flows. Interestingly, the decrease in the thickness of the boundary layer for the system with the narrower gap is higher, as is seen from the data at US intensities higher than 18 W/cm^2. Finally, for both electrode gaps, a minimum diffusion layer thickness (δ_{min}) of 10 μm is reached as the ultrasound power is raised. It has been suggested that this is mainly due to the limiting conversion of ultrasound energy to turbulent liquid flow (Marken et al., 1996). In all cases shown in Fig. 4a–c, the values of δ achieved with US are more than a third of the δ under silent conditions, which shows the usefulness of such agitation.

In order to examine more deeply into the mechanism of US agitation at the electrode surface, Sherwood number correlations were developed. For this purpose, a value of flow velocity, U, far away from the electrode is required. The flow velocity (U) of the jet of ultrasound waves flowing between the electrodes at different ultrasound power densities was estimated using the relationship formulated by Eklund et al. (1996), which is shown in Fig. 2. The

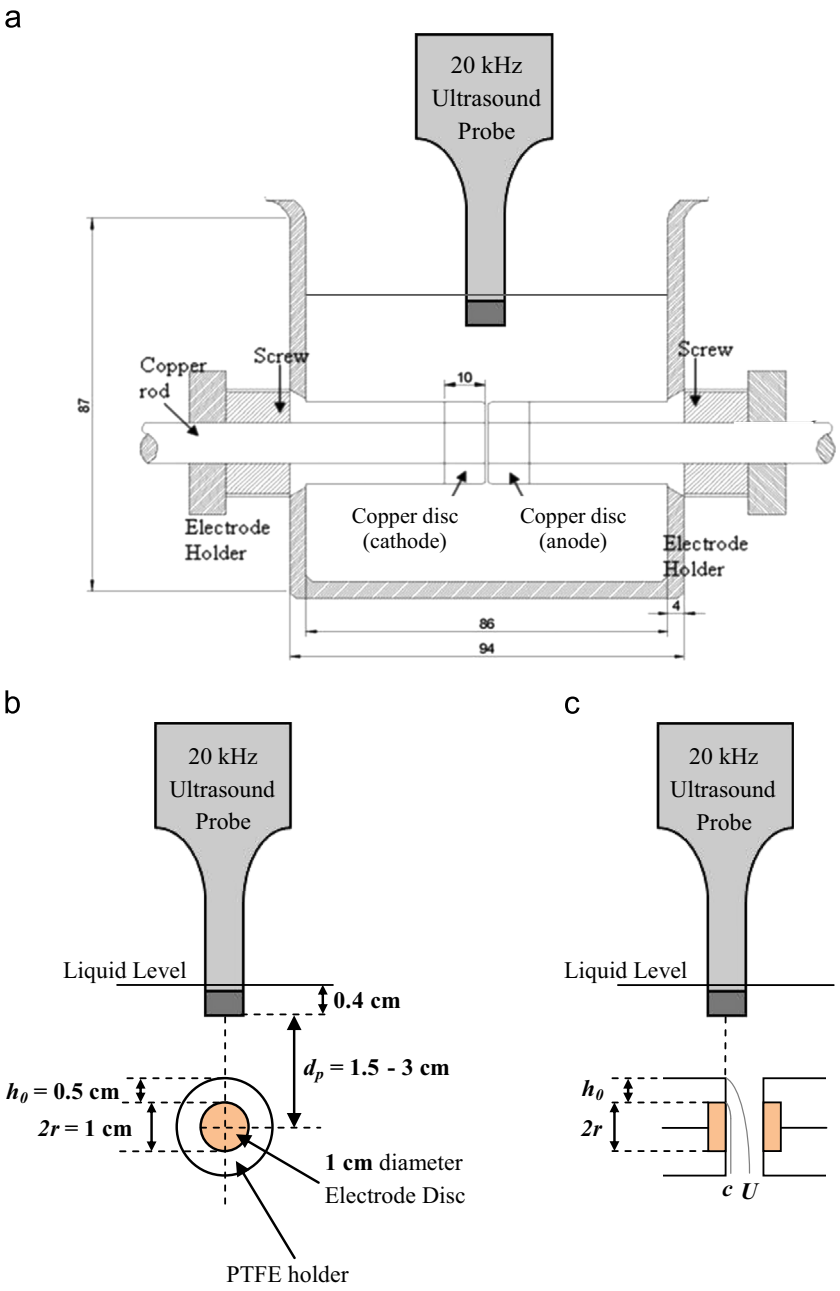

Fig. 3. (a) Experimental set-up of the electrochemical cell used in this work with ultrasound probe placed directly above the narrow electrode gap; (b) position of probe in solution above the working electrode, with the variable parameter d_p. (c) Side view of placement of probe, with concentration (c) and flow velocity (U) profiles demonstrating the development of the momentum and concentration boundary layers.

value of Reynolds number, *Re*, was calculated using $Re=(Ud_H)/\nu$, with the values of U shown in Fig. 2. The *Re* numbers for the range of ultrasound powers examined in our experiments were found to be approximately 700–2000 and 2700–7400 for the small and large gaps, respectively, as shown in Table 2 in Appendix.

Sherwood–Schmidt–Reynolds numbers correlations for copper deposition are calculated for electrode gaps of 0.15 cm and 1 cm, shown in Fig. 6. The line of best-fit in Fig. 6 gave the correlations displayed in Eqs. (6) and (7) for electrode gaps of 1 cm and 0.15 cm respectively.

$$Sh = 1.7 \times 10^{-3}\left(Re\,Sc\,\frac{d_e}{L}\right)^{0.82} \tag{6}$$

$$Sh = 9 \times 10^{-6}\left(Re\,Sc\,\frac{d_e}{L}\right)^{1.38} \tag{7}$$

These correlations can be compared against standard mass transfer correlations obtained for forced convection flow between two parallel electrodes, displayed in Eq. (3). The value of b for the 1 cm electrode gap is ~0.8, showing the onset of turbulent flow. However, the turbulent flow becomes fully developed when the electrode gap is narrowed to 0.15 cm, illustrated by the value of b of ~1.4 in Eq. (7). It is suggested that this is possibly due to the formation of eddies at the top of the narrower gap, which could occur when the turbulent jet of ultrasound waves come into contact with the top section of the electrode holder.

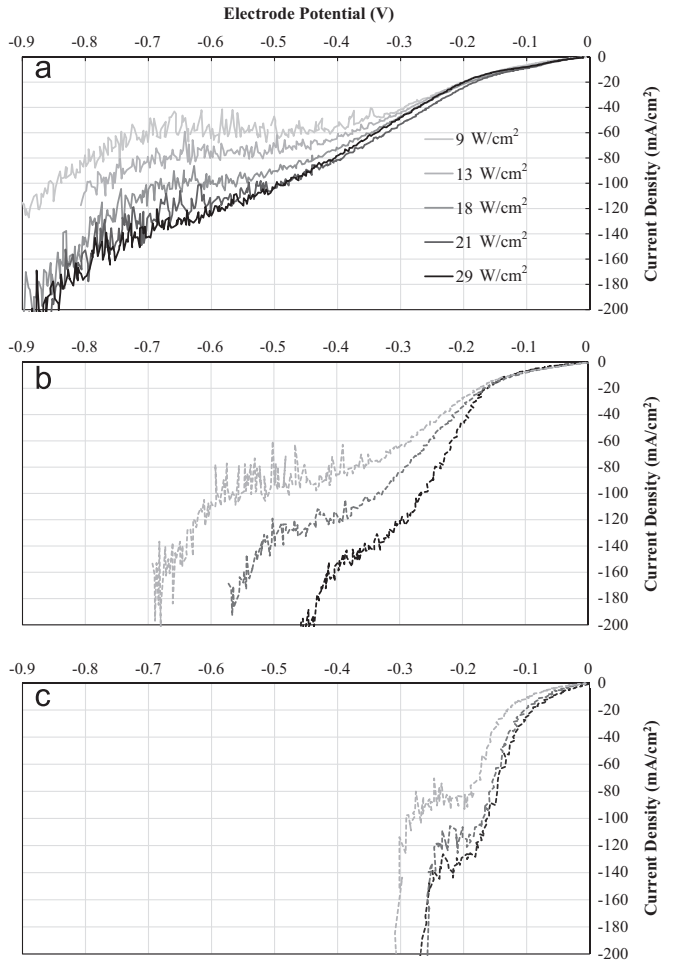

Fig. 4. Linear Potential scans with a 0.1 M $CuSO_4$+0.1 M H_2SO_4 electrolyte; Scan Rate=5 mV/s. (a) at varying ultrasound intensities (9–29 W/cm^2), h_e=1 cm; d_p=3 cm. (b) h_e=0.5 cm; at varying d_p of 3 cm (dashed light grey), 2 cm (dashed grey) and 1.5 cm (dashed black) at fixed p of 18 W/cm^2. (c) h_e=0.15 cm, with same ultrasound conditions as for 'b' and varying d_p at distances of 3 cm (dashed light grey), 2 cm (dashed grey) and 1.5 cm (dashed black).

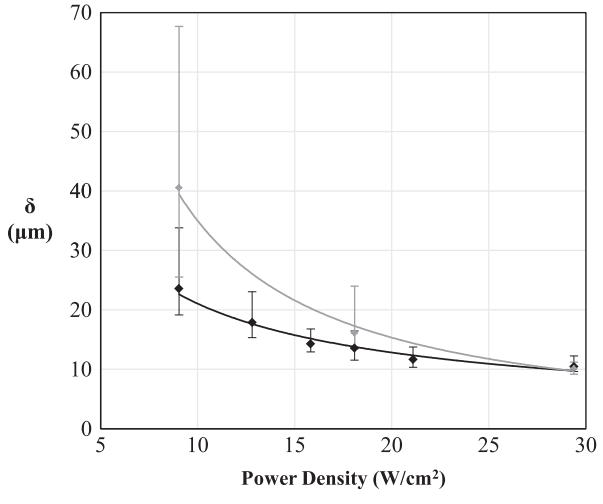

Fig. 5. Diffusion layer thickness (δ) calculated using experimental limiting currents and Eq. (5) as a function of US power density. h_e=0.15 cm (grey), 1 cm (black); d_p=3 cm.

It is significant that the *Sh* correlation shows fully developed turbulence for the narrower gap, which means that the efficacy of US is higher even though the *Re* values are smaller. For example, at 29 W/cm^2, the *Re* for the small and large gap is 2000 and 7400, respectively, but the value of δ is virtually the same. The turbulence in the narrower gap may be induced by the interaction between the US waves and the edges of the parallel electrodes leading to eddy formation, which needs to be investigated further.

Table 1
Calculated change in potential at the cathode surface for varying electrode gaps and probe distances.s

Change in probe distance, d_p (cm)	Change in electrode gap, h_e (cm)	Change in potential at cathode (V)
3–1.5	1 (constant)	+0.130
3–1.5	0.15 (constant)	+0.085
3 (constant)	1–0.15	+0.135
1.5 (constant)	1–0.15	+0.090
3 to 1.5	1–0.15	+0.220

Table 2
Calculated Reynolds numbers at varying powers for two difference electrode gaps, with values of U at each power, obtained from Fig. 2.

Electrode gap (cm)	Power (W/cm^2)	Velocity, U (cm/s)	*Re*
1	9	27	2686
	18	48	4795
	29	75	7430
0.15	9	27	701
	18	48	1251
	29	75	1938

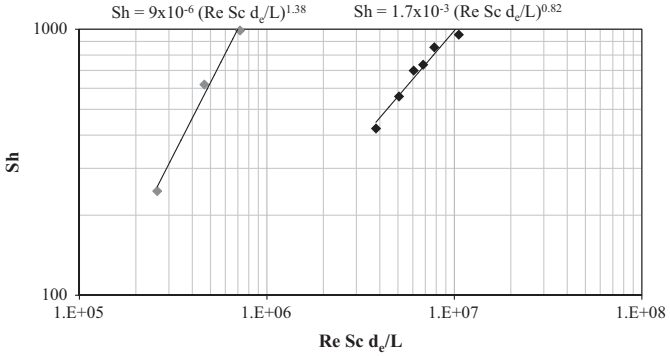

Fig. 6. Mass transfer correlations using US agitation. Data shown for US power 18 W/cm^2 and probe–electrode distance of 3 cm, where the US source is far away from the electrode. Inter-electrode gaps of 0.15 cm (grey) and 1 cm (black).

5. Discussion

A noticeable issue in this work was the difficulty in detecting a limiting current plateau when the electrodes were placed close to each other or when the distance between the probe and electrode was lowered. Although current oscillations have been observed in a variety of US investigations (Compton et al., 1996a; Eklund et al., 1996; Marken et al., 1996) using both side-on and face-on geometries, there is less information on distortions in polarisation data during electrochemical reactions. Marken and Compton (1996) have mentioned that current can flow to the US probe itself, since it is metallic, and has also suggested methods of obviating this problem; including bipotentiostatic control and electrically insulating the probe. However, bipotentiostats are not used in industry and therefore cannot be used for all applications, and electrically insulting the probe may lower the ultrasound

power. Polarisation data of other researchers have also shown that limiting current plateau is not observed during US agitation (Reisse et al., 1994). In our case, it can be seen in Fig. 4c, that the plateaux region is very small. This means that the limiting current technique may have only limited applicability for measuring mass transfer limitations for electrochemical systems using US.

In order to examine more deeply into the apparent distortion in potential measurement, further analysis was carried out. There is a possibility that the probe is acting as an earth relative to the electrodes. However, Marken and Compton (1996) suggest that an ultrasound probe placed within an electrolyte solution of an electrochemical cell can act as a second working electrode; therefore the surface of the probe was modelled as a second cathode. A primary current distribution model of copper electrodeposition was carried out using a commercial electrodeposition software, ElSyca (ElSy, SA) using a two dimensional model of the cell in Fig. 3. The software was used to determine if the potential at which the hydrogen evolution region begins could shift from −0.6 V to −0.3 V as the electrode gap is decreased from 0.5 to 0.15 cm at a probe distance of 3 cm, as was observed in the polarisation experiment shown in Fig. 4.

The calculation used for the model assumed that there is a uniform concentration gradient of ions in the solution and also constant electrolyte conductivity. The well-known equation for the flux of an ionic species k (N_k) was used, shown in Eq. (8).

$$N_k = -D_k\nabla c_k + c_k v - z_k u_k F c_k \nabla\phi \tag{8}$$

where u_k is the mobility of species k (cm^2mol/J s) and $\nabla\phi$ is the potential gradient (V). The accumulation of species k can be expressed as the equation shown in Eq. (9).

$$\frac{\partial c_k}{\partial t} = -\nabla\cdot N_k + R_k \tag{9}$$

where R_k is the production rate of species k (mol/s). A more convenient mass balance equation can be written as Eq. (10), derived by substituting Eq. (8) into Eq. (9).

$$\frac{\partial c_k}{\partial t} + v\cdot\nabla c_k = z_k F\nabla(u_k c_k\nabla\phi) + \nabla(D_k\nabla c_k), \quad k = 1....n \tag{10}$$

The velocity of an incompressible fluid flow in electrochemical systems is described by the well-known Navier–Stokes equation, with constant density and viscosity

$$\nabla\cdot v = 0 \tag{11}$$

The electric potential (Φ) in an electrochemical system can be expressed using the Poisson equation, shown in Eq. (12). However, this can be replaced with the electroneutrality expression in Eq. (13) due to the condition that the bulk electrolyte solution is electrically neutral.

$$\nabla^2\phi = -\frac{F}{\epsilon}\sum_k^n z_k c_k \tag{12}$$

$$\sum_k^n z_k c_k = 0 \tag{13}$$

where ϵ is the dielectric constant of the solution (Farad/m). The current density can then be described by Eq. (14). If N_k is substituted by Eq. (8), then the current density can be expressed in terms of diffusion, convection and migration. If the conductivity (σ) is taken into account (Eq. (13)), along with the condition of electroneutrality (Eq. (15)), then the current density can be given by Eq. (16).

$$i = F\sum_k^n z_k N_k \tag{14}$$

$$\sigma = F^2\sum_k^n z_k u_k c_k \tag{15}$$

$$i = -\sigma\nabla\phi - F\sum_k^n z_k D_k\nabla c_k \tag{16}$$

For steady-state conditions, Eq. (10) can be omitted. If there is a continuous stirring of the solution, it can be assumed that convection is dominant and concentration gradients can be omitted, therefore Eq. (10) can be simplified to Eq. (17), the well-known Laplace equation. This means that the current density can be expressed as Eq. (18).

$$\sigma\nabla^2\phi = 0 \tag{17}$$

$$i = -\sigma\nabla\phi \tag{18}$$

This model is solved using the Boundary Element Method in ElSyca, using the boundary conditions that the current density at each point at the insulating walls of the cell and the top surface of the solution is zero. This means that the current flows to the electrodes only; in this case the anode, cathode as well as the US probe placed in solution

$$i_y = i\cdot 1_y = -\sigma\nabla\phi\cdot 1_y = -\sigma\frac{\partial\phi}{\partial y} \tag{19}$$

$$\frac{\partial\phi}{\partial y} = 0 \tag{20}$$

where y denotes the normal distance from the surface.

A constant temperature of 293 K was used and the electrolyte conductivity used was 59.8 mS/cm. The dimensions of the US probe were modelled as a rectangle with a width and of height 1.3 cm, 0.4 cm respectively, placed above the electrode gap. 30 elements were used on both the cathode and anode, 120 elements on the surface of the probe facing the electrodes and 30 elements on the side of the probe. The convergence of the current density calculation was achieved when the current residual reached a value of <0.001 mA/cm^2 and the calculation was completed within 6 iterations (at maximum number of iterations of 20).

Typical results from the modelling analysis are presented in Fig. 7. The potential isolines for electrode gaps of 1 cm and 0.15 cm with the ultrasound probe at probe–electrode distances of 3 cm and 1.5 cm are shown in the figure. The results show that due to the presence of a large metallic probe, significant distortion in the potential field occurs. As the electrodes are brought closer together or when the probe is brought closer to the two electrodes the distortion in the field is greater and current begins to flow to the probe, as proposed by Marken and Compton (1996). This resulted in copper deposition on the probe surface, observed during our polarization experiments. The current flow from the top of the anode to the probe surface meant that smaller current densities were calculated at the top section of the cathode surface in the modelling. This would therefore be the cause of deposit thickness non-uniformity along the cathode length.

The change in potential at the cathode at different probe distances and electrode gaps is displayed in Table 1. Interestingly, the cathode potential can shift by 0.085–0.22 V in the positive direction depending on the proximity of the US probe and the two different electrodes. This shift in potential is of a similar magnitude to the shift in potential observed experimentally in Fig. 4, which explains the differences in polarisation data acquired for the different electrode geometries. Both narrowing the electrode gap and lowering the probe result in potential distortions which shorten the current plateaux, and also causes current to flow through the probe. This measured limiting current is therefore inaccurate, depending on the distance between the probe and the electrodes. Our modelling data showed that 17% of the total current flowed to the probe for the smallest probe to electrode distance. These findings therefore show that within very

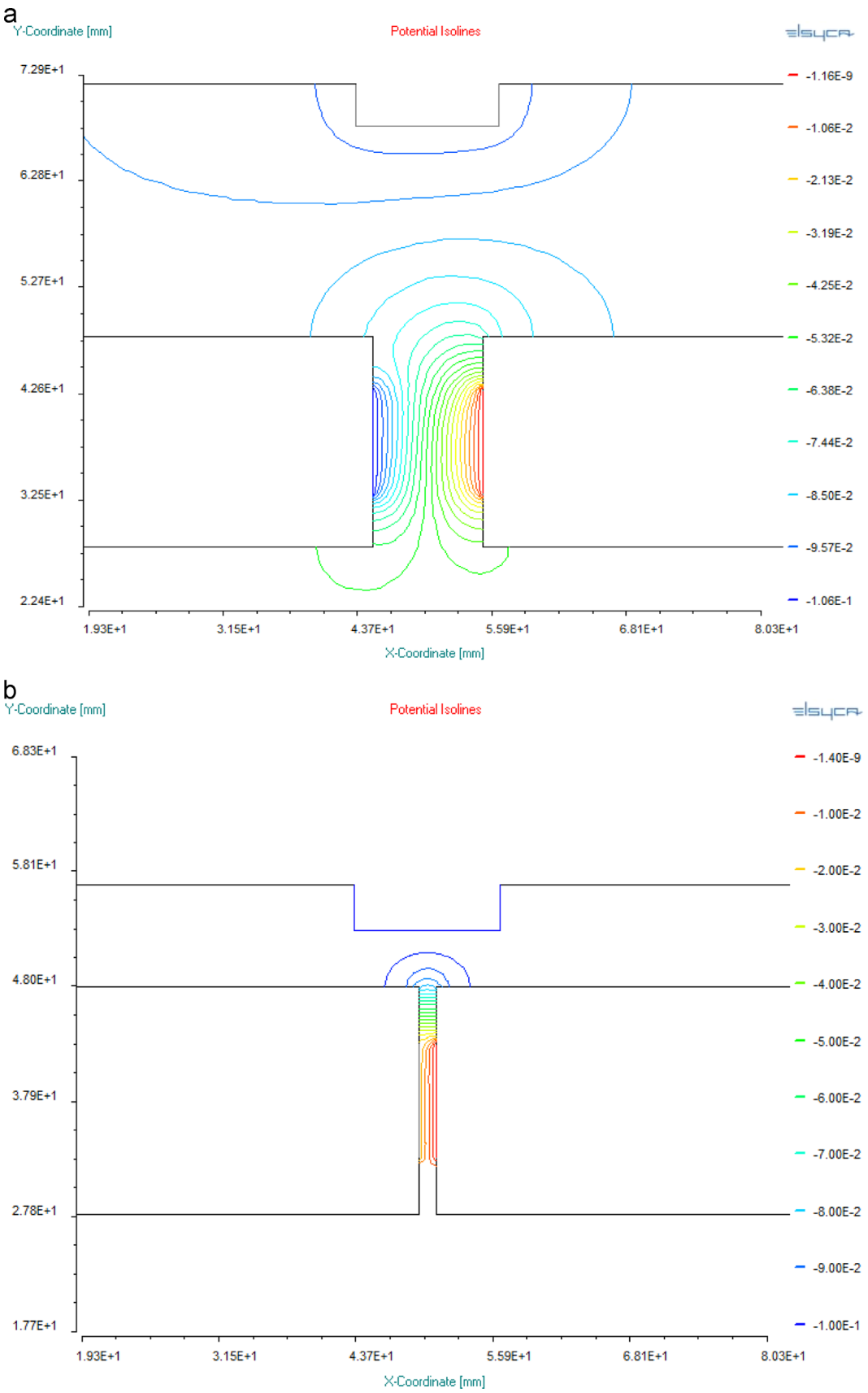

Fig. 7. Potential isolines within the electrochemical cell with an ultrasound probe placed in the electrolyte solution with cathode (left) and anode (right). Potential applied = −0.1 V. (a) h_e = 1 cm; d_p = 3 cm. (b) h_e = 0.15 cm; d_p = 1.5 cm.

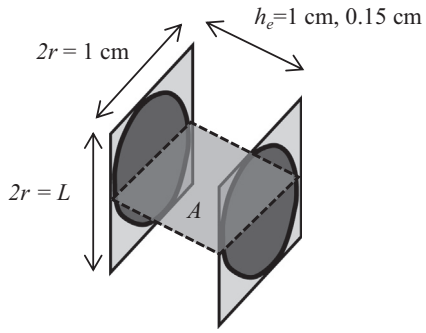

Fig. 8. Schematic of electrode gap for calculation of d_H with assumption of square electrodes. $2r$=Characteristic length, A=cross-sectional area, h_e=electrode gap.

constricted geometries, the employment of the limiting current technique may be limited.

6. Conclusions

The effect of a side-on ultrasound probe on the mass transfer during copper deposition at narrow inter-electrode gaps was investigated. The limiting current technique was used to determine the diffusion layer thickness, which were then used to determine mass transfer correlations. It was found that ultrasonic agitation significantly improved mass transfer, with the ability to increase limiting currents by a factor of 10.

Ultrasound powers of 9–18 W/cm^2 were found to provide more effective agitation. As expected, stirring at the electrode surface increased as the US probe was brought into closer proximity to the electrodes. Sherwood correlations showed that turbulent flows were present near the electrode surface when a side-on probe is used. For larger inter-electrode spacing the developing turbulence was observed, whereas for narrow electrode gaps fully turbulent correlations were obtained.

Polarisation data for copper deposition were found to be distorted when the metallic US probe was brought closer to the electrodes, and when the anode and cathode were in close proximity. A current distribution analysis showed that the distortion in polarisation data was caused by the close placement of the metallic US probe to the two parallel electrodes. These findings hold implications for limiting current analyses used to study mass transfer within narrow electrode gaps in a horizontal regime or within concentric cylindrical electrodes in close proximity to each other (Coeuret and Legrand, 1981), as well as for other ultrasonic applications where the source of ultrasound has to be placed in close proximity to a substrate or work piece.

Nomenclature

Φ	potential (V)
a	constant coefficient in Sherwood correlation
A	cross-sectional area of channel between the electrodes (cm^2)
b	exponent in Sherwood correlation
c	concentration (mol/cm^3)
d	distance (cm)
D	diffusivity (cm^2/s)
δ	diffusion layer thickness (cm)
h_e	electrode gap (cm)
ϵ	dielectric constant of the solution (Farad/m)
F	Faraday constant (96485 A s/mol)
Gr	Grashof Number (dimensionless)
h_0	distance between the leading edge of the momentum and the concentration boundary layers (cm)
i	current density (mA/cm^2)
I	current (mA)
L	characteristic length (cm)
N	flux of species (mol/cm^{2}s)
ν	kinematic viscosity (cm^2/s)
p	ultrasound power intensity (W/cm^2)
σ	conductivity (S/m)
r	radius (cm)
Re	Reynolds Number, dimensionless
R	production rate (mol/s)
Sc	Schmidt number, dimensionless
Sh	Sherwood number, dimensionless
t	time (s)
U	limiting solution velocity at a larger distance from the plate (cm/s)
u	mechanical mobility of species k (cm^{2}mol/J.s)
w	electrode width (cm)
x	length along the electrode from the edge closest to the probe (cm)
z	charge of species

Subscripts

b	bulk
e	equivalent (diameter) (cm)
H	hydraulic (diameter) (cm)
k	species
Lim	Limiting
min	minimum
p	distance from probe tip to the centre of the electrode surface (cm)
$sono$	in the presence of ultrasonic agitation

Acknowledgements

Simon Coleman acknowledges the studentship support by EPSRC, UK grant EP/J500288/1. This work was supported by EU "MESMOPROC" Grant 303550. The Chemical Engineering workshop is acknowledged for cell fabrication.

Appendix

Reynolds number calculations

The electrode dimensions were simplified to 1 cm square electrodes for the dimensionless analysis, shown in the schematic in Fig. 8. The hydraulic diameter (d_H) was calculated using the equation $d_H=4A/(4r+2h_e)$, where A is the cross-sectional area of the channel between the electrodes, r is the radius of the electrode and h_e is the electrode gap.

References

Coeuret, F., Legrand, J., 1981. Mass transfer at the electrodes of concentric cylindrical reactors combining axial flow and rotation of the inner cylinder. Electrochim. Acta 26 (7), 865–872.

Compton, R.G., Eklund, J.C., Page, S.D., Mason, T.J., Walton, D.J., 1996a. Voltammetry in the presence of ultrasound: mass transport effects. J. Appl. Electrochem. 26, 775–784.

Compton, R.G., Gooding, J.G., Sokirko, A., 1996b. Chronoamperometry at Channel Electrodes: analytical theory of transient behaviour at double electrodes. J. Appl. Electrochem. 26, 463–469.

Cottrell, F.G., 1903. Residual current in galvanic polarization, regarded as a diffusion problem. Z. Phys. Chem. 42, 385.
Doraiswamy, A., Dunaway, T.M., Wilker, J.J., Narayan, R.J., 2009. Inkjet printing of bioadhesives. J. Biomed. Mater. Res. Part B: Appl. Biomater. J. Biomed. Mater. Res. Part B: Appl. Biomater. 89B, 28–35.
Eklund, J.C., Marken, F., Waller, D.N., Compton, R.G., 1996. Voltammetry in the presence of ultrasound: a novel sono-electrode geometry. Electrochem. Acta 41 (9), 1541–1547.
Fenech, E.J., Tobias, C.W., 1960. Mass transfer by free convection at horizontal electrodes. Electrochim. Acta 2, 311–325.
Fouad, M.G., Ibl, N., 1960. Natural convection mass transfer at vertical electrodes under turbulent flow conditions. Electrochimica Acta. 3, 233–243.
Franssila, S., 2010. Introduction to Microfabrication, 2nd ed. Wiley, West Sussex.
Kuhn, A., Argoul, F., 1995. Diffusion-limited kinetics in thin-gap electroless deposition. J. Electroanal. Chem. 397 (1–2), 93–104.
Levich, V.G., 1962. Physicochemical hydrodynamics. Prentice-Hall, New Jersey, pp. 87–91.
Lorimer, J.P., Pollet, B., Phull, S.S., Mason, T.J., Walton, D.J., Geissler, U., 1996. The effect of ultrasonic frequency and intensity upon limiting currents at rotating disc and stationary electrodes. Electrochem. Acta 41 (17), 2737–2741.
Madou, M.J., 2012. 3rd ed.Fundamentals of Microfabrication and Nanotechnology, vol. 2. CRC Press, Boca Raton.
Maisonhaute, E., White, P.C., Compton, R.G., 2001. Surface Acoustic Cavitation understood via nanosecond electrochemistry. J. Phys. Chem. B 105 (48), 12087–12091.
Marken, F., Compton, R.G., 1996. Electrochemistry in the presence of ultrasound: the need for bipotentiostatic control in sonovoltammetric experiments. Ultrason. Sonochem. 3 (1), S131–S134.
Marken, F., Akkermans, R.P., Compton, R.G., 1996. Voltammetry in the presence of Ultrasound: the limit of acoustic streaming induced diffusion layer thinning and the effect of solvent viscosity. J. Electroanal. Chem. 415 (1), 55–63.
Mason, T.J., Lorimer, J.P., 2002. Applied Sonochemistry: Uses of Power Ultrasound in Chemistry and Processing. Wiley, Weinheim.
Meuleman, W.R.A., Roy, S., 2003. Transient electrochemical processes during Cu-Ni deposition. Trans. Inst. Metal Finish. 81, 55–58.
Nouraei, S., Roy, S., 2008. Electrochemical process for micropattern transfer without photolithography: a modeling analysis. J. Electrochem.. Soc. 155 (2), D97–D103.
Ohsaka, T., Goto, Y., Sakamoto, K., Isaka, M., Imabayashi, S., Hirano, K., 2010. Effect of intensities of ultrasound sonication on reduction of crack formation and surface roughness in iridium electrodeposits. Trans. Inst. Metal Finish. 88 (4), 206.
Ramachandran, R., Saraswathi, R., 2009. Sonoelectrochemical studies on mass transport in some standard redox systems. Rus. J. Electrochem. 47 (1), 15–25.
Reisse, J., Francois, H., Vandercammen, J., Fabre, O., Kirchch-de Mesmaeker, A., Maerschalk, C., Delplanke, J.-L., 1994. Sonoelectrochemistry in aqueous electrolyte: a new type of sonoelectroreactor. Electrochim. Acta 39, 37–39.
Richardson, K.A., de Groot, P.A.J., Lanchester, P.C., Birkin, P.R., Barltent, P.N., 1997. Towards the electrochemical manufacture of superconductor precursor films in the presence of an ultrasonic field. J. Electroanal. Chem. 420 (1), 22.
Rosso, M., Chassaing, E., Chazalviel, J.N., Gobron, 2002. Onset of current driven concentration instabilities in thin cell electrodeposition with small inter-electrode distance. Electrochem. Acta 47, 1267–1273.
Roy, S., Gupte, Y., Green, T.A., 2001. Flow cell design for metal deposition at recessed circular electrodes and wafers. Chem. Eng. Sci. 56 (17), 5025–5035.
Roy, S., 2007. Fabrication of micro- and nano-structured materials using mask-less processes. J. Phys. D: Appl. Phys. 40, 413–416.
Samarasinghe, S.R., Pastoriza-Santos, I., Edirisinghe, M.J., Reece, M.J., Liz-Marzan, L.M., 2006. Printing gold nanoparticles with an electrohydrodynamic direct-write service. Gold Bull. 39, 48–53.
Sand, H.J.S., 1901. On the concentration at the electrodes in a solution with special reference to the liberation of hydrogen by electrolysis of a mixture of copper sulphate and sulphuric acid. Philol. Mag. 1, 45–79.
Schonenberger, I., Roy, S., 2005. Microscale pattern transfer without photolithography of substrates. Electrochim. Acta 51 (1), 809–819.
Texier, F., Servant, L., Bruneel, J.L., Argoul, F., 1998. in situ probing of interfacial processes in the electrodeposition of copper by confocal Raman microspectroscopy. J. Electroanal. Chem. 446, 189–203.
Tobias, C.W., Hickman, R.G., 1965. Z. Phys. Chem. 229, 145.
Tolmachev, Y.V, Wong, Z., Scherson, D.A., 1996. Theoretical aspects of laminar flow in a channel-type electrochemical cell as applied to in-situ attenuated total reflection-infrared spectroscopy. J. Electrochem. Soc. 143, 3160–3166.
Wagner, C., 1949. The role of natural convection in electrolytic processes. Trans. Am. Electrochem. Soc. 95, 61.
Walton, D.J., Phull, S.S., Chyla, A., Lorimer, J.P., Mason, T.J., Burke, L.D., Murphy, M., Compton, R.G., Eklund, J.C., Page, S.D., 1995. Sonovoltammetry at platinum electrodes: surface phenomena and mass transport processes. J. Appl. Electrochem. 25, 1083–1090.
Whitaker, J.D., Nelson, J.B., Schwarts, D.T., 2005. Electrochemical printing: software reconfigurable electrochemical microfabrication. J. Micromech. MicroEng. 15 (8), 1498–1503.
Widayatno, T., Roy, S., 2011. Electrodeposition of nickel pattern without photolithography of substrates. In: Proceedings of 3rd International Congress on Green Process Engineering (GPE), Kuala-Lumpur, Malaysia, 6–8 November, 2011.
Wragg, A.A., 1971. Combined free and forced convective ionic mass transfer in the case of opposed flow. Electrochim. Acta 16, 373.
Wragg, A.A., Ross, T.K., 1967. Superposed free and forced convective mass transfer in an electrochemical flow system. Electrochim. Acta 12, 1421.
Wu, Qi-Bai, Green, T.A., Roy, S., 2011. Electrodeposition if microstructures using patterned anode. Electrochem. Commun. 13 (11), 1229–1232.
Yeager, E., Hovorka, F., 1953. Ultrasonic Waves and Electrochemistry. I. A survey of the electrochemical applications of ultrasonic waves. J. Acoust. Soc. Am. 25 (3), 444.
Yu, H., Bologen, O., Li, B., Murrat, T.W., Zhang, J., 2006. Fabrication of three-dimensional microstructures based on singled-layered SU-8 for lab-on-chip applications. Sens. Actuators A 127, 228–234.
Zelinsky, A.G., Pirogov, B.Y., 2009. Electrolysis in a closed Electrochemical cell with a small inter-electrode distance. Metal dissolution/deposition in plain electrolyte. Electrochem. Acta 54, 6707–6712.